RSC Advances

ROYAL SOCIETY OF CHEMISTRY

www.rsc.org/advances

A reliable self-assembled peptide based electrochemical biosensor for detection of caspase 3 activity and apoptosis

Balal Khalilzadeh[a], Nasrin Shadjou[b], Morteza Eskandani[a], Hojatollah Nozad Charoudeh[d,e], Yadollah Omidi[a,c], and Mohammad-Reza Rashidi[a,c,*]

[a] *Research Center for Pharmaceutical Nanotechnology (RCPN), Tabriz University of Medical Sciences, Tabriz, Iran*

[b] *Department of Nanochemistry and Nanotechnology Center, Urmia University, Urmia, Iran*

[c] *Faculty of Pharmacy, Tabriz University of Medical Sciences, Tabriz, Iran*

[d] *Stem Cell Research Center, Tabriz University of Medical Sciences, Tabriz, Iran*

[e] *Faculty of Medicine, Tabriz University of Medical Sciences, Tabriz, Iran*

Corresponding author E-mail: rashidi@tbzmed.ac.ir

Abstract

A sensitive electrochemical self-assembled peptide based biosensor was developed for detection of caspase 3 activity and apoptosis using Asp-Glu-Val-Asp (DEVD) modified peptide and horseradish peroxidase (HRP) as cleaving and electron transfer (current amplifier) agents, respectively. Streptavidin coated magnetic beads (MB) was used to increase the loading efficiency of HRP on the DEVD modified peptide. The electrochemical behaviors were investigated by cyclic, linear sweep and square wave voltammetry techniques. The results were also further evaluated by electrochemical impedance spectroscopy. The experimental conditions influencing caspase 3 analysis were optimized in terms of buffer pH, hydrogen peroxide concentration, incubation time and ratio of MB to HRP. The limit of detection (LOD) of the designed biosensor was found as 100 pM. The proposed biosensor was successfully applied to determine caspase 3 activity in human lung cancer cells treated with doxorubicin which suggests that the biosensor could be applicable for analysis of caspase 3 activity and detection of apoptosis in real samples.

Keywords: electrochemical biosensor, caspase 3 activity, horseradish peroxidase, magnetic bead, apoptosis detection, DEVD modified peptide

1. Introduction

Self-assembled monolayers (SAMs) are patterned, flexible and thin layers of organic molecules which have a "headgroup" with a specific affinity for a substrate in their structures. These materials can be formed by spontaneous adsorption of liquid or gas phases on the surfaces of noble metals, metal oxides and semiconductors substrates. The ease of formation and functionalization, reasonable stability for extended period, organization into well-ordered arrays and affinity to metal substrates, make SAMs ideal model systems in many fields including fabrication of electrochemical sensors and biosensors. The most widely studied systems of SAMs are derived from the adsorption of alkanethiols on gold surface. The adsorption of thiolated molecules on gold substrates are achieved *via* adlayer model of the Au-S bonding interactions. The binding of the biological recognition elements to the gold surface can be achieved through formation of SAMs of thiol groups with suitable reactive groups (such as the amine group of a peptide or protein) on one end of the molecule and the gold-complexing thiol on the other. This makes alkanethiols as excellent candidates for preparation of biosensors for biomarker analysis [1-5]. Cysteine terminated peptides are among biomolecules that can react with gold substrates *via* covalent bonds (sulphur-gold bond) producing peptide based self-assembled monolayers (PBSAMs). PBSAMs can act as an electron transition bridge between organic layer and electrode surface [6-10].

Caspases are cysteine-dependent proteases and can modify numerous endogenous proteins through proteolytic cleavage at a cysteine amino acid followed by an aspartic acid residue [11-13]. Accordingly, these proteases are involved in various physiological and pathological processes such as inflammation, necrosis and cancer, and play the most important role in apoptotic pathways. Cells undergoing apoptosis are characterized by a series of distinct morphological and

biochemical changes including activation of caspases. The apoptotic caspases are categorized into different types including caspase 3. Caspase 3 is the most frequently activated death protease during the early stage of apoptosis making this key mediator as a well-established cellular marker of apoptosis. It is also of particular interest in cancer research, development of the central nervous system and cell differentiation process in stem cell growing steps. Accordingly, sensitive detection of caspase 3 activity has become an important subject in not only apoptosis diagnosis but also detection of therapy efficiency and the evaluation of the biological function and disease progression [14-19]. Caspase 3 is able to specially and accurately cleavage the N-terminal of tetra motive sequence (Asp-Glu-Val-Asp, DEVD). Thereupon, scientists used this sequence cleavage for detecting of caspase 3 activity [20, 21]. Many analytical techniques, particularly based on nanostructure materials or nano labeling, have been used for quantification of caspase 3 activity including electrochemical [20-24], optical [25-34], imaging [35, 36], flow cytometry [37], atomic force microscopy [38] and magnetic resonance imaging [39]. However, in spite of having many advantages, these methods could be expensive, time-consuming, labor-intensive, or use toxic chemicals and require sophisticated instrumentation and highly technical expertise. To achieve a more sensitive, selective and convenient detection method for caspase 3 activity, a novel electrochemical biosensor was developed in the present study to detect caspase 3 activity. In this study, DEVD modified peptide was casted on Au surface using self-assembled method. Then, the active surface of gold electrode was blocked by 6-mercapto-1-hexanol (MCH) and the electrode was incubated with streptavidin coated magnetic bead (MB) followed by incubation of the electrode with biotinylated horseradish peroxidase (B-HRP) for 1 h at 37ºC. To our best knowledge, this is the first report of using streptavidin coated magnetic bead and biotinylated horseradish peroxidase (B-HRP) for detection of caspase 3 activity with

electrochemical technique. In some biosensors developed for caspase 3 detection, toxic materials such as cadmium[21] and p-nitroaniline[23] have been used. However, the biosensor fabricated in the present study has the advantage of using no toxic compounds alongside other advantages such as ability of miniaturization, user-friendly, low detection limit and short response time.

2. Experimental

2.1 Chemical and reagents

All chemicals were analytical grade and used without further purifications. The biotinylated peptide (Biotin-G-D-G-D-E-V-D-G-C) was obtained from Peptron Company, Korea (98.57%, molecular weight 1092) containing DEVD sequence. Streptavidin coated magnetic beads (Dynabeads® MyOne Streptavidin T1, (MB)) and biotinylated HRP were purchased from Invitrogen (Carlsbad, CA, USA). Hydrogen peroxide, H_2O_2 (30%), 6-mercapto-1-hexanol (MCH), hydroquinone (HQ) and doxorubicin hydrochloride (DOX) were obtained from Sigma-Aldrich. Recombinant human caspase 3 was purchased from R&D (Minneapolis, MN, USA). Caspase 3 activity kit was obtained from BD biosciences (Bedford, MA, USA). Tris (2-carboxyethyl) phosphine hydrochloride (TCEP) was purchased from Bio basic Inc (Markham, Ontario, Canada). Phosphate buffered saline, PBS (0.01 M) was prepared by dissolving appropriate amount of NaCl, KCl, Na_2HPO_4 and KH_2PO_4 in a 1.0 L volumetric flask. Sodium acetate buffer was prepared by dissolving appropriate quantity of glacial acetic acid and sodium acetate. Concentrated solutions of sodium hydroxide and hydrochloric acid were used to adjust optimum pH. Cell lyse buffer was produced with dissolving appropriate amount of NaCl, Tris (hydroxymethyl) aminomethane hydrochloride, ethylenediaminetetraacetic acid disodium salt, triton X-100 and sodium dodecyl sulfate. All buffer solutions were sterilized by autoclave and

filtered throw 0.2 μm filter. All electrochemical experiments were carried out at room temperature.

2.2 Apparatus and procedures

All cyclic voltammetry (CV), square wave voltammetry (SWV), linear sweep voltammetry (LSV) and electrochemical impedance spectroscopy (EIS) experiments were performed on an AUTOLAB electrochemical system, PGSTAT302N (Eco Chemie, Utrecht, Netherlands). The system was run on a PC using NOVA 1.8 and FRA software. HRP-MB-biotinylated peptide modified Au electrode, Pt wire and Ag/AgCl (satd.) 3 M KCl were used as working, counter and reference electrodes, respectively. SWV experiments were performed by step potential of 0.005 V, amplitude of 0.02 V, interval time 0.04 S and the scan rate of 0.125 V/S. FACS flow cytometry experiments was performed with Becton-Dickinson fluorescence activated cell sorter, BD FACSCalibur^{TM} (BD Biosience, San Jose, USA) using Cell Quest pro software provided by the BD company. Total protein concentrations were balanced with nanodrop spectrophotometer (ND-1000, USA).

2.3 Preparation of caspase 3 biosensor

The Au electrode (2 mm diameter) was rinsed with double distillated water. Then, the Au electrode was soaked in piranha solution and polished with 0.03 μm alumina powder. In this step, to remove adsorbed particles, the electrode was sonicated in double distilled water and ethanol, respectively. Finally, the electrode was dried with nitrogen stream. 2 mM solution of biotinylated peptide (BP) was prepared in sodium acetate buffer (pH=5.2); the mentioned buffer

was deoxygenated with slow argon stream. To prevent formation of disulphide bonds at the C-terminal of the biotinylated peptide, the prepared biotinylated peptide solution was activated with appropriate amount of TCEP solution. This procedure was done for 1 hour accomplished by mixing of solution, each 15 min, at room temperature [21]. Then, 25 µl of 2 mM activated biotinylated peptide was poured on the dried Au electrode and the modification was performed at 4ºC for 12 hour with 100% humidity. After that, the modified electrode was rinsed with PBS (pH=6.5) for 10 min. To block nonspecific adsorption of the peptide chain and abundant non-target proteins in cell lysates on the gold surface [21] and also to get stable and reproducible currents, the modified electrode was immersed in 1 mM MCH solution for 1 hour at room temperature and then rinsed again with PBS (pH=6.5) for 10 min. Subsequently, 20 µl of streptavidin coated magnetic beads (MB) was incubated with 30 µl of biotinylated HRP at 37ºC for 1 hour with 100% humidity while mixing (up and down) of the solution each 15 min. The conjugated MB and biotinylated HRP was washed 3 times with PBS (pH=7.4, FBS 1%) using Invitrogen magnet (DynaMag™-2 Magnet) [40-42]. After that, 5 µl of the conjugated MB and biotinylated HRP was spread on the biotinylated peptide modified electrode and incubated at 37ºC for 1 hour with 100% humidity. Then, the completely modified electrode was washed with PBS (pH=6.5) for 10 min and used as sensitive biosensor for detection of caspase 3 activity in extracted proteins of A549 cell lines treated with DOX. Overlay, the designed biosensor relies on the decrease in the reduction current of HQ in the presence of H_2O_2 and HRP due to the cleavage of the DEVD modified peptide by caspase 3. The electrode preparation steps and the detection process have been illustrated in Scheme 1.

2.4 Cell culture

Adenocarcinomic human alveolar basal epithelial A549 cells obtained from Pasteur Institute of Iran were used as model. The cells were cultured in media containing Roswell Park Memorial Institute (RPMI) at a seeding density of 30×10^4 with penicillin (100 IU)/streptomycin (100 µg/ml), 10% fetal bovine serum, in an incubator with humidified atmosphere containing 95% air and 5% CO_2 at 37°C.

2.5 Induction of apoptosis

After reaching about 60-80% confluency, the cells were washed with PBS (pH=7.4) and treated with different concentrations of DOX diluted in complete media. Then, the cells were allocated in two groups: group A for FACS study and group B for biosensor assay. After 48 h, the cells were washed with PBS (pH=7.4) and exposed to trypsin for 3 min at 37°C. The excess trypsin was deactivated by addition of fetal bovine serum containing media. The suspended cells, then, were centrifuged at 1000 rpm for 5 min at 25°C, collected and counted. The activity of caspase 3 enzyme of different treatments were measured using KIT according to the supplier instruction. Briefly, the cells were washed twice with wash buffer, then, exposed to permeabilization buffer, incubated at 4°C followed by washing with PBS and incubation with caspase 3 monoclonal antibody conjugated with R-phycoerythrin (R-PE) for 30 min at room temperature. R-PE is an algae based red protein-pigment complex and is commonly used as fluorochrome (λ_{ex}=488 nm, λ_{em}=575 nm) in flow cytometery. After final washing step, the cells were analyzed by flow cytometry.

2.6 Total protein extraction

For the biosensing study, the total proteins of the treated and untreated cells of the second group were extracted using cell lyses protocol. Briefly, the attached cells were trypsinated, washed with PBS (pH=7.4) and centrifuged at 1000 rpm for 8 min at 4°C. After, the cells were incubated on ice pack for at least 5 min and then 200 µl lyse buffer was added. Then, the cells were incubated at 4°C for 1 hour, and finally centrifuged at 12000 rpm for 20 min at 4°C and the supernatants were collected. The protein concentration of all extracted groups was measured using nanodrop and the same amount of protein exactly were handled to the next step for detecting of caspase 3 activity with designed biosensor.

3. Results and discussion

3.1 Cyclic voltammetry and Electrochemical Impedance Spectroscopy of the prepared peptide based biosensor

Preparation steps of proposed biosensor was studied using CV and EIS techniques in PBS (pH=6.5) containing HQ and H_2O_2. In Fig.1A, the CVs of biosensor in the individual steps of preparation have been illustrated. As can be seen in Fig. 1A, in the case of bare Au electrode, no oxidation or reduction peak in PBS appeared. But, immediately after addition of HQ to the buffer solution, two small peaks were observed at 0.53 V (oxidation) and -0.067 V (reduction). At the second stage, modification of the Au electrode with biotinylated peptide (BP) was performed and two redox peaks appeared at 0.059 V and -0.002 V. Then, blocking of the remaining binding sites of gold surface was carried out using MCH. This led to a little decrease in the oxidation peak currents because of the shielding effect of MCH. Subsequent modification with MBs was

performed and the CV was recorded. Due to conductivity of MBs, both oxidation and reduction peak currents increased. Final modification step was carried out with biotinylated HRP in which HRP acts in electron transfer mechanism and HQ as an excellent electron mediator is used to improve electron transfer between HRP and electrode. Therefore, high reduction peak current was obtained after modification of MB-DEVD-Au electrode with HRP. Obtained results by CV were confirmed by EIS. Fig. 1C and D illustrates the EIS curves of biosensor in different preparation steps. As the obtained Nyquist plot of EIS was not enough clear, the phase bode of EIS was used for comparison and evaluation of the different steps used for the preparation of the biosensor. In Fig. 1B, phase bode of EIS studies has been shown.

3.2 Electrochemical behavior of prepared biosensor:

3.2.1 Cyclic Voltammetry (CV), square wave voltammetry (SWV) and linear sweep voltammetry (LSV)

Electrochemical behavior of HRP-MB-DEVD-Au electrode was studied using cyclic voltammetry (CV) in the presence of HQ as electroactive species and H_2O_2 as HRP activator. Fig. 2A shows CVs of HRP-MB-DEVD-Au electrode in the presence of HQ (curve b) and after injection of H_2O_2 (curve c) in PBS (pH 6.5). As shown in Fig. 2A, the electrochemical reduction peak current of HQ increased immediately after addition of H_2O_2. The increment of reduction peak current of HQ confirms that the electrode preparation steps are correct and the assembled HRP on the surface of HRP-MB-DEVD-Au electrode is active. These results were further confirmed by SWV. As can be seen in Fig. 2B, there is no signal in PBS (pH=6.5) (curve a); but, one sharp oxidation peak was appeared after addition of 300 µl of 0.04 M HQ (Fig. 2B curve b).

Finally, following injection of H_2O_2, the oxidation peak of HQ was raised confirming that the biosensor has been prepared correctly. Loaded HRP on modified electrode was used to transfer electron between modified electrode, electroactive media (HQ) and H_2O_2. The results obtained were similar to those reported by others [40]. Electron transfer mechanism has been summarized in reactions 1-3:

$$HRP(Fe^{3+}) + H_2O_2 \rightarrow HRP\ (Fe^{4+}) + H_2O \quad (1)$$

$$HRP(Fe^{4+}) + HQ_{(RED)} \rightarrow HRP\ (Fe^{3+}) + HQ_{(OX)} \quad (2)$$

$$HQ_{(OX)} + 2H^+ + 2e^- \rightarrow HQ_{(RED)} \quad (3)$$

Electrochemical reduction behavior of HQ was also studied with LSV on HRP-MB-DEVD-Au electrode in PBS (0.01M, pH=6.5). According to reaction 3, HQ is reduced in the presence of HRP *via* H_2O_2. Therefore, after addition of H_2O_2, the reduction peak current of HQ highly increased, subsequently H_2O_2 activates the HRP protein with oxidation of its ferric ion [43](Fig. 2C).

The effect of scan rate on CV behavior of HRP-MB-DEVD-Au electrode was performed in PBS (0.01 M, pH=6.5) in the presence of 1 mM HQ and 1.5 mM H_2O_2. CVs of HRP-MB-DEVD-Au electrode were investigated in various potential sweep rates from 2 to 1000 mVs^{-1}. It can be seen in Fig. 3A, with increments of scan rates from 2 to 1000 mVs^{-1}, the oxidation and reduction peaks currents of HQ increased. In addition, HQ showed two pairs of redox peaks on HRP-MB-DEVD-Au electrode. Additionally, Fig. 3A shows two oxidation peaks that appeared at 0.08 V (Peak I) and 0.5V (Peak II), while the reduction peaks were observed at 0.43 V (Peak III) and -0.07 V (Peak IV) (Fig. 3A). The relation between oxidation and reduction peak currents *versus*

square root of the potential sweep rate has been illustrated in Fig. 3B. According to this figure, the mass transfer process is a diffusion controlled phenomena. On the other hand, Fig. 3B shows that with an increase in the scan rates, the peaks current of I and IV are markedly elevated. Based on these results, peaks I and IV were selected as candidate peaks for the next investigations. The results were further confirmed by Tafel plot. Based on Tafel plot[44], variation of peak potential can be recorded *versus* Napierian logarithm of peak currents (Fig. 3C). According to equation 1, the slop was 18.222, consequently, β is equal to 0.4679. While β is closer to 0.5, therefore, mass transfer process is diffusion controlled [44].

$$Ln\ Ip = constant + \left(\beta\left(\frac{F}{RT}\right)\right)Ep \quad (1)$$

In addition, by recording of peak currents *vs.* scan rates (Fig. 3D), special surface coverage (Γ^*) can be obtained using equation 2 [44]:

$$Ip = \left(\frac{n^2F^2}{4RT}\right)\upsilon A\Gamma^* \quad (2)$$

where, n is number of transferred electron, F is Faraday's constant, R is Gas constant, T is temperature in kelvin scale, υ is potential sweep rate, A is total electrode surface and Γ^* is special surface covered with HRP-MB-DEVD-Au electrode [44]. The special surface coverage with HRP-MB-DEVD-Au electrode was 1.69×10^{-9} mol cm^{-2}. By the compartment of this result (special surface coverage) with the previously reported work, it is found that HRP-MB-DEVD-Au electrode has wide active surface area [20]. It is important to point out that the surface coverage of the peptide on our gold electrode was much higher than that reported by others [20].

3.3 Optimization of parameters:

3.3.1 Effect of pH

Linear sweep voltammetry was chosen as an electrochemical technique for investigating of pH effect on electrochemical response of the modified electrode in PBS. Both acidic and basic media (5.5, 6, 6.5, 7, 7.3, 8, 8.5 and 9.5) was selected for pH optimization. Variation of peak currents in different pHs of buffer solution was illustrated in Fig. 4A. The results show that the peak currents increased from 5.5 to 6.5 and then, decreased until reach to 9.5. The higher response current was appeared nearby pH=6.5. Therefore, pH=6.5 was selected as an optimum pH. Variation of peak currents vs. pH of buffer solutions were shown in Fig. 4B. According to recent studies [45, 46], the enzymatic reaction of HRP and HQ are highly rely on the pH of solution.

3.3.2 Incubation time effect

The effect of incubation time on the electrochemical response of HRP-MB-DEVD-Au electrode was investigated in A549 cell lysate using LSV. Fig. 4C demonstrates the LSVs of HRP-MB-DEVD-Au electrode in A549 cell lysate at different incubation times. Obtained results from Fig. 4C shows that with increasing incubation time, the reduction peak currents decreased. Therefore, it is found that after 60 min incubation, the peak currents reach a plateau. Variation of peak currents vs. incubation times were shown in Fig. 4D. As a result, 60 min incubation time was chosen as optimum incubation time.

3.3.3 Optimization of H_2O_2

The effect of H_2O_2 concentration on the electrochemical response of HRP-MB-DEVD-Au electrode was examined with CV, in the presence of 100 µL of 0.04M HQ. Fig. 5A shows the plot of peak currents versus H_2O_2 concentration. According to this figure, the peak currents of

HRP-MB-DEVD-Au electrode increase by increasing H_2O_2 concentration to 1.15 mM followed by a decrease in the peak currents. Same results for H_2O_2 concentration effect on HRP in the presence of HQ have been reported before [47]. Therefore, 1.15 mM H_2O_2 was selected as optimum concentration of H_2O_2.

3.3.4 Optimization of MB and biotinylated HRP

Optimization of MB and biotinylated HRP was performed with CV. For this task, different concentrations of biotinylated HRP were incubated with MB. In Fig. 5B and 5C, cyclic voltammogram and plot of the effect of biotinylated HRP concentration on constant concentration of MB has been presented respectively. As it can be seen in Fig. 5C, the highest peak currents are achieved by 7.5 µl of biotinylated HRP. Accordingly, the ratio of MB to biotinylated HRP was selected as 5 to 7.5 µL. These results are consistent with those reported previously [40].

3.3.5 TCEP effect on peak current

According to previous studies [21], the biotinylated peptide (Biotin-G-D-G-D-E-V-D-G-C) has cysteine in its structure and in solution phase, two cysteine terminated peptides might be coupled each other and make disulfide bonds between them. Furthermore, disulfide bonds are interfering agents and should be reduced. It has been proved that TCEP is a suitable agent for reduction of disulfide bonds. Thus, concentrations effect of TCEP on electrochemical response of HRP-MB-DEVD-Au electrode were investigated by CV technique. Accordingly, 12.8 µL 10 mM TCEP was selected as the optimum amount for subsequent optimization steps.

3.4 Electroanalytical performance of the peptide based biosensor

Electroanalytical performance of HRP-MB-DEVD-Au electrode was investigated using SWV technique. For this purpose, different concentrations of caspase 3 were incubated with HRP-MB-DEVD-Au electrode for 1 hour. Fig. 6A shows the SWVs of HRP-MB-DEVD-Au electrode in different concentrations of caspase 3. The peak at ≈0.4 V was selected for the SWV analysis. SWV voltammograms showed that the peak current decreases as concentrations of caspase 3 increase (Fig. 6A and 6B) which can be attributed to the cleavage of HRP-MB-DEVD by caspase 3 and release of the HRP molecule from the electrode surface. This, in turn, can cause a decrease in the peak current. The cleavage behavior of designed peptide versus different concentrations of caspase 3 is not linear which is consistent with other reports [23, 27, 28, 33, 34, 48]. According to the results obtained, it was possible to apply this technique to the quantitative analysis of caspase 3 activity. Calibration curve was illustrated in Fig. 6B. Relative standard deviation (RSD) of the HRP-MB-DEVD-Au electrode in the presence of HQ and H_2O_2 with 20 repetitive analysis was calculated as 0.83%. Stability of the proposed electrode was also tested in PBS for 24 h using SWV. No significant difference was obtained on peak current of caspase 3. The performance of the designed electrochemical caspase 3 biosensor in comparison with other techniques has been presented in Table 1.

3.5 Fluorescence activated cell sorting (FACS) analysis:

FACS analysis which is extensively used for apoptosis detection was employed to validate the applicability of the developed biosensor for the analysis of apoptosis or caspase 3 activity in lung cancer cell line as a biological sample. Lung cancer cells were treated with different

concentrations of DOX for induction of apoptosis. The cells were divided into four groups. The first group was cultured in media without DOX and used as negative control group. Three other groups were cultured with media containing 0.5, 2.5 nM and 32 μM of DOX (as positive control groups), corresponding cells pictures were taken by invertor microscope in Fig. 7A, 7B, 7C and 7D respectively. Then, the cells were analyzed by flow cytometry according to the method described by caspase 3 Kit supplier. The results obtained from A549 treated and untreated cells analysis by SWV and FACS methods have been shown in Figs. 6C and 8, respectively. The FACS analysis was not able to detect any caspase 3 activity in either the negative control group or the cells treated with 0.5 and 2.5 nM DOX. However, the newly developed biosensor could differentiate between these groups in terms of apoptosis induction. Therefore, the engineered peptide-based biosensor is more sensitive than the FACS method in measurement caspase 3 activity and detection of apoptosis.

4. Conclusions

In the present work, a sensitive and simple peptide-based biosensor (HRP-MB-DEVD-Au electrode) was developed for the detection and determination of caspase 3 activity and the biosensor was successfully used to measure caspase 3 activity in apoptotic cell lines. In this newly developed electrochemical biosensor, HRP labeled streptavidin coated magnetic beads was used as electron transfer agent. Reduction of HQ by HRP on the HRP-MB-DEVD-Au electrode was used for quantification of caspase 3 activity with SWV technique. Depending on the caspase 3 activity, the peptide was cleaved and the current decreased. Using this method, it was possible to measure apoptosis and caspase 3 activity with LOD value of 100 pM. The application of the engineered biosensor for caspase 3 activity was tested on A549 cell line, which

was used as real sample cell model induced by doxorubicin. In addition, it seems that the HRP-MB-DEVD-Au electrode could be used as a suitable biosensing platform for pharmaceutical and biological analysis.

Acknowledgments

The authors gratefully acknowledge for the financial support of this project by Research Center for Pharmaceutical Nanotechnology (RCPN) at Tabriz University of Medical Sciences. This project was a part of PhD thesis (number 92/014/125/3) and its grant number was 92001.

References:

1. M. Delvaux, A. Walcarius and S. Demoustier-Champagne, *Biosensors and Bioelectronics*, 2005, **20**, 1587-1594.
2. S. Ferretti, S. Paynter, D. A. Russell, K. E. Sapsford and D. J. Richardson, *TrAC Trends in Analytical Chemistry*, 2000, **19**, 530-540.
3. N. Islam, F. Shen, P. V. Gurgel, O. J. Rojas and R. G. Carbonell, *Biosensors and Bioelectronics*, 2014, **58**, 380-387.
4. J. C. Love, L. A. Estroff, J. K. Kriebel, R. G. Nuzzo and G. M. Whitesides, *Chemical Reviews*, 2005, **105**, 1103-1170.
5. M. H. a. Y. O. Mehdi Jaymand, *Progress in Polymer Science*, 2015, 10.1016/j.progpolymsci.2014.1011.1004.
6. M. Goel, E. N. G. Marsh, Z. Chen and N. L. Abbott, *Langmuir*, 2014, **30**, 7143-7151.
7. M. Venanzi, E. Gatto, M. Caruso, A. Porchetta, F. Formaggio and C. Toniolo, *The Journal of Physical Chemistry A*, 2014, **118**, 6674-6684.
8. H. Li, Y. Huang, B. Zhang, X. Pan, X. Zhu and G. Li, *Analytical Chemistry*, 2014, **86**, 12138-12142.
9. H. Li, H. Xie, Y. Cao, X. Ding, Y. Yin and G. Li, *Analytical Chemistry*, 2013, **85**, 1047-1052.
10. H. Li, H. Xie, Y. Huang, B. Bo, X. Zhu, Y. Shu and G. Li, *Chemical Communications*, 2013, **49**, 9848-9850.
11. K. M. Boatright and G. S. Salvesen, *Current Opinion in Cell Biology*, 2003, **15**, 725-731.
12. Y. Fuchs and H. Steller, *Cell*, 2011, **147**, 1640.
13. H. Mehmet, *Nature*, 2000, **403**, 29-30.
14. D. E. Christofferson and J. Yuan, *Current Opinion in Cell Biology*, 2010, **22**, 263-268.
15. S. Haupt, M. Berger, Z. Goldberg and Y. Haupt, *Journal of Cell Science*, 2003, **116**, 4077-4085.
16. M. O. Hengartner, *Nature*, 2000, **407**, 770-776.
17. K. Itoh, H. Hase, H. Kojima, K. Saotome, K. Nishioka and T. Kobata, *Rheumatology*, 2004, **43**, 277-285.
18. V. N. Ivanov, A. Bhoumik and Z. e. Ronai, *Oncogene*, 2003, **22**, 3152-3161.

19. J. Yuan and G. Kroemer, *Genes & Development*, 2010, **24**, 2592-2602.
20. H. Xiao, L. Liu, F. Meng, J. Huang and G. Li, *Analytical Chemistry*, 2008, **80**, 5272-5275.
21. J.-J. Zhang, T.-T. Zheng, F.-F. Cheng and J.-J. Zhu, *Chemical Communications*, 2011, **47**, 1178-1180.
22. P. Miao, J. Yin, L. Ning and X. Li, *Biosensors and Bioelectronics*, 2014, **62**, 97-101.
23. S. Takano, S. Shiomoto, K. Y. Inoue, K. Ino, H. Shiku and T. Matsue, *Analytical Chemistry*, 2014, **86**, 4723-4728.
24. S. Zhou, T. Zheng, Y. Chen, J. Zhang, L. Li, F. Lu and J.-J. Zhu, *Biosensors and Bioelectronics*, 2014, **61**, 648-654.
25. K. Boeneman, B. C. Mei, A. M. Dennis, G. Bao, J. R. Deschamps, H. Mattoussi and I. L. Medintz, *Journal of the American Chemical Society*, 2009, **131**, 3828-3829.
26. H. Chen, Q. Mei, Y. Hou, X. Zhu, K. Koh, X. Li and G. Li, *Analyst*, 2013, **138**, 5757-5761.
27. Y. Pan, M. Guo, Z. Nie, Y. Huang, Y. Peng, A. Liu, M. Qing and S. Yao, *Chemical Communications*, 2012, **48**, 997-999.
28. M. S. Rahman, T. Kabashima, H. Yasmin, T. Shibata and M. Kai, *Analytical Biochemistry*, 2013, **433**, 79-85.
29. H. Shi, R. T. K. Kwok, J. Liu, B. Xing, B. Z. Tang and B. Liu, *Journal of the American Chemical Society*, 2012, **134**, 17972-17981.
30. H. Wang, Q. Zhang, X. Chu, T. Chen, J. Ge and R. Yu, *Angewandte Chemie International Edition*, 2011, **50**, 7065-7069.
31. J. Zhang, X. Wang, W. Cui, W. Wang, H. Zhang, L. Liu, Z. Zhang, Z. Li, G. Ying, N. Zhang and B. Li, *Nat Commun*, 2013, **4**.
32. Z. Gu, A. Biswas, K.-I. Joo, B. Hu, P. Wang and Y. Tang, *Chemical Communications*, 2010, **46**, 6467-6469.
33. D. E. Prasuhn, A. Feltz, J. B. Blanco-Canosa, K. Susumu, M. H. Stewart, B. C. Mei, A. V. Yakovlev, C. Loukou, J.-M. Mallet, M. Oheim, P. E. Dawson and I. L. Medintz, *ACS Nano*, 2010, **4**, 5487-5497.
34. V. Gurtu, S. R. Kain and G. Zhang, *Analytical Biochemistry*, 1997, **251**, 98-102.
35. P. Ray, A. De, M. Patel and S. S. Gambhir, *Clinical Cancer Research*, 2008, **14**, 5801-5809.
36. Y.-w. Jun, S. Sheikholeslami, D. R. Hostetter, C. Tajon, C. S. Craik and A. P. Alivisatos, *Proceedings of the National Academy of Sciences*, 2009, **106**, 17735-17740.
37. J. M. Cárdenas-Maestre, A. M. Pérez-López, M. Bradley and R. M. Sánchez-Martín, *Macromolecular Bioscience*, 2014, **14**, 923-928.
38. T. Kihara, C. Nakamura, M. Suzuki, S.-W. Han, K. Fukazawa, K. Ishihara and J. Miyake, *Biosensors and Bioelectronics*, 2009, **25**, 22-27.
39. S. Mizukami, R. Takikawa, F. Sugihara, Y. Hori, H. Tochio, M. Wälchli, M. Shirakawa and K. Kikuchi, *Journal of the American Chemical Society*, 2007, **130**, 794-795.
40. B. V. Chikkaveeraiah, A. A. Bhirde, N. Y. Morgan, H. S. Eden and X. Chen, *ACS Nano*, 2012, **6**, 6546-6561.
41. V. Mani, B. V. Chikkaveeraiah, V. Patel, J. S. Gutkind and J. F. Rusling, *ACS Nano*, 2009, **3**, 585-594.
42. B. A. Otieno, C. E. Krause, A. Latus, B. V. Chikkaveeraiah, R. C. Faria and J. F. Rusling, *Biosensors and Bioelectronics*, 2014, **53**, 268-274.
43. B. V. Chikkaveeraiah, V. Mani, V. Patel, J. S. Gutkind and J. F. Rusling, *Biosensors and Bioelectronics*, 2011, **26**, 4477-4483.
44. A. J. Bard and L. R. Faulkner, *Hoboken: Wiley and Sons*, 2001.
45. J. Wu, F. Yan, J. Tang, C. Zhai and H. Ju, *Clinical Chemistry*, 2007, **53**, 1495-1502.

46. Z.-M. Liu, Y. Yang, H. Wang, Y.-L. Liu, G.-L. Shen and R.-Q. Yu, *Sensors and Actuators B: Chemical*, 2005, **106**, 394-400.
47. H. Qi, C. Ling, Q. Ma, Q. Gao and C. Zhang, *Analyst*, 2012, **137**, 393-399.
48. L. Jixiang, M. Bhalgat, C. Zhang, D. Zhenjun, B. Hoyland and D. H. Klaubert, *Bioorganic & Medicinal Chemistry Letters*, 1999, **9**, 3231-3236.

Figures captions:

Scheme 1: Illustration of electrode preparation steps

Figure 1: **A**) Cyclic voltammograms, **B**) bode phase curves, **C**) Nyquist curves and **D**) The enlarged part of EIS of HRP-MB-DEVD-Au electrode in presence of 1 mM HQ and 1.5 mM Hydrogen peroxide in PBS (pH=6.5) at bare au, bare au+BP, bare Au+BP+MCH, bare Au+BP+MCH+MB, bare Au+BP+MCH+MB+HRP.

Figure 2: **A**) Cyclic voltammograms, **B**) Square wave voltammograms at the frequency of 25 Hz. Amplitude is 0.02 V. interval time is 0.04 s and **C**) Linear sweep voltammograms of HRP-MB-DEVD-Au electrode in the absence (a) and presence of 1 mM HQ (b) and 1 mM HQ + 1.5 mM H_2O_2 (c) at the scan rate of 100 mV/s.

Figure 3: **A**) Cyclic voltammograms of HRP-MB-DEVD-Au electrode at different scan rates (2, 4, 6, 8, 10, 20, 30, 40, 50, 60, 70, 80, 90, 100, 150, 200, 250, 300, 350, 400, 450, 500, 550, 600, 650, 700, 750, 800, 850, 900, 950 and 1000 mV/s), **B**) Variation of peak currents *versus* square root of scan rate using HRP-MB-DEVD-Au electrode, **C**) Variation of Napierian logarithm of peak currents *versus* peak potentials of HRP-MB-DEVD-Au electrode at the scan rate of 10 mV/s, and **D**) Variation of peak currents *versus* scan rate (30, 40, 50, 60, 70, 80, 90 and 100 mV/s) using HRP-MB-DEVD-Au electrode, in the presence of 1 mM HQ and 1.5 mM Hydrogen peroxide.

Figure 4: **A**) Linear sweep voltammograms of HRP-MB-DEVD-Au electrode in different pH of buffer solutions (5.5, 6.0, 6.5, 7.0, 7.3, 8.0, 8.5 and 9.5), **B**) Variation of peak currents vs. pH of buffer solutions, **C**) Linear sweep voltammograms of HRP-MB-DEVD-Au electrode in different incubation times (10, 30, 40, 60, 75 and 120 min) and **D**) variation of peak currents vs. incubation times.

Figure 5: **A**) Variation of reduction peak currents *versus* H_2O_2 concentrations in PBS (pH 6.5). HQ concentration is 1 mM, **B**) Cyclic voltammograms of HRP-MB-DEVD-Au electrode in different incubation amounts (2.5, 5, 7.5, 15, 20, 30 and 50 µL) of biotinylated HRP on 5 µL MB and **C**) Variation of peak currents vs. different concentrations of biotinylated HRP.

Figure 6: **A**) Square wave voltammograms of HRP-MB-DEVD-Au electrode before and after 1 hour incubation time with 0.0, 0.1, 0.5 and 1 nM caspase 3 concentrations in the presence of 0.76 mM HQ and 1 mM Hydrogen peroxide, **B**) Variation of peak currents *versus* different concentrations of caspase 3, and **C**) Square wave voltammograms of HRP-MB-DEVD-Au electrode before and after 1 hour incubation time in the extracted total proteins of A549 cell lines with negative, 0.5, 2.5 nM and 32 µM DOX treated groups

Figure 7: The pictures of A549 cell lines with negative (A), 0.5 nM (B), 2.5 nM (C) and 32 µM (D) DOX treated groups.

Figure 8: FACS flow cytometry analyses of A549 cell lines with negative (A), 0.5 nM (B), 2.5 nM (C) and 32 μM (D) DOX treated groups

Table 1: Performance comparison of the designed biosensor with other techniques*

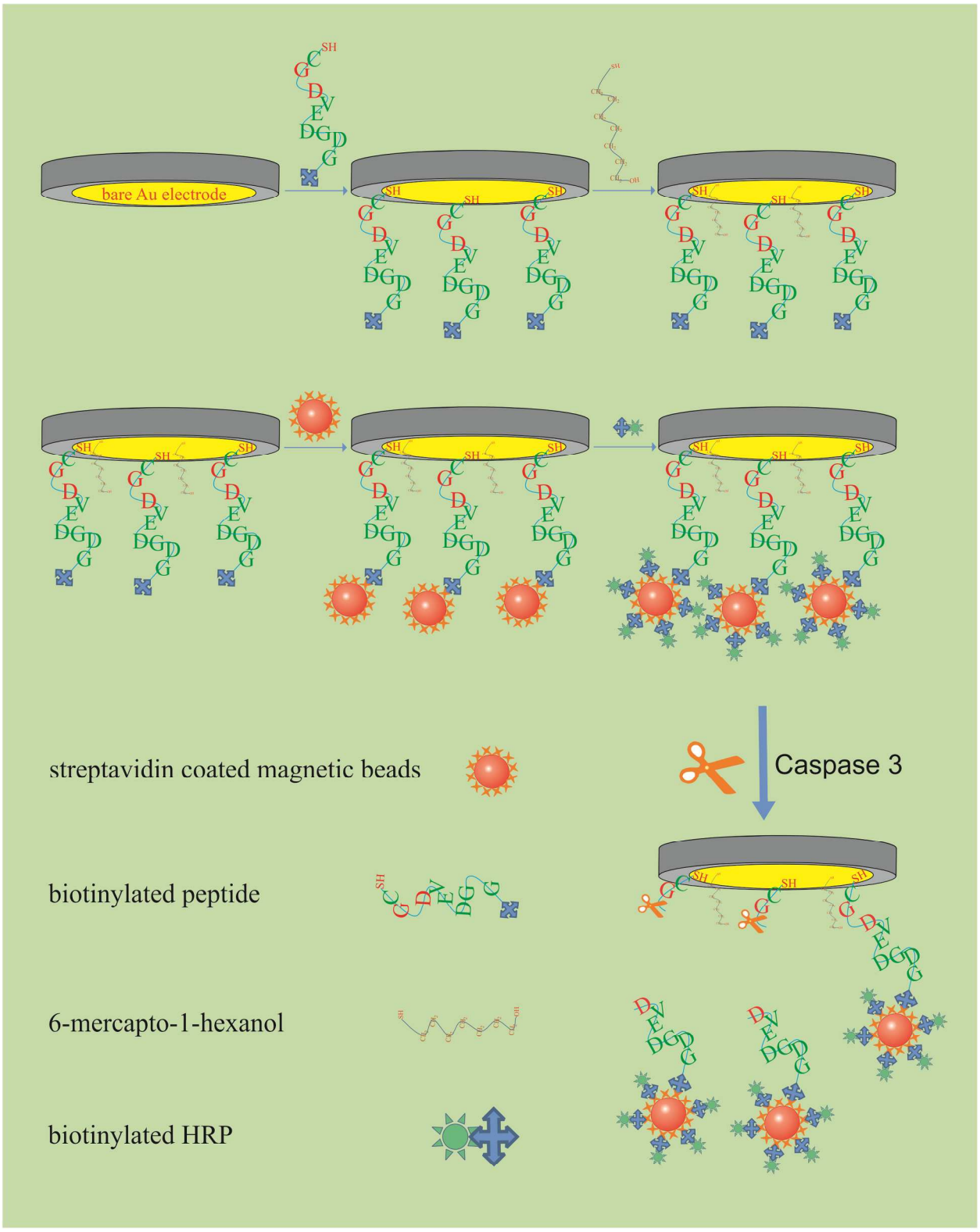

Scheme 1

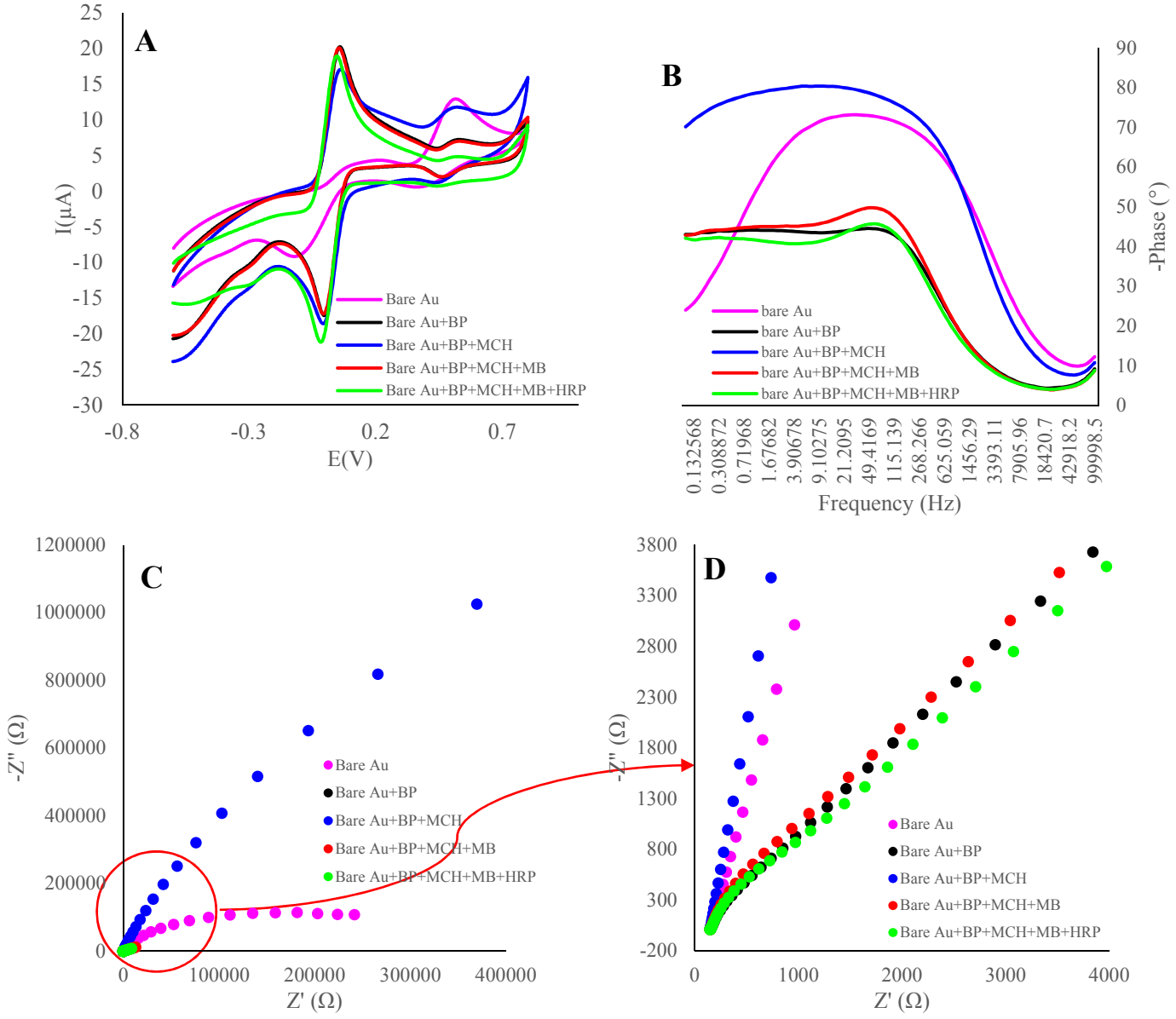

Figure 1

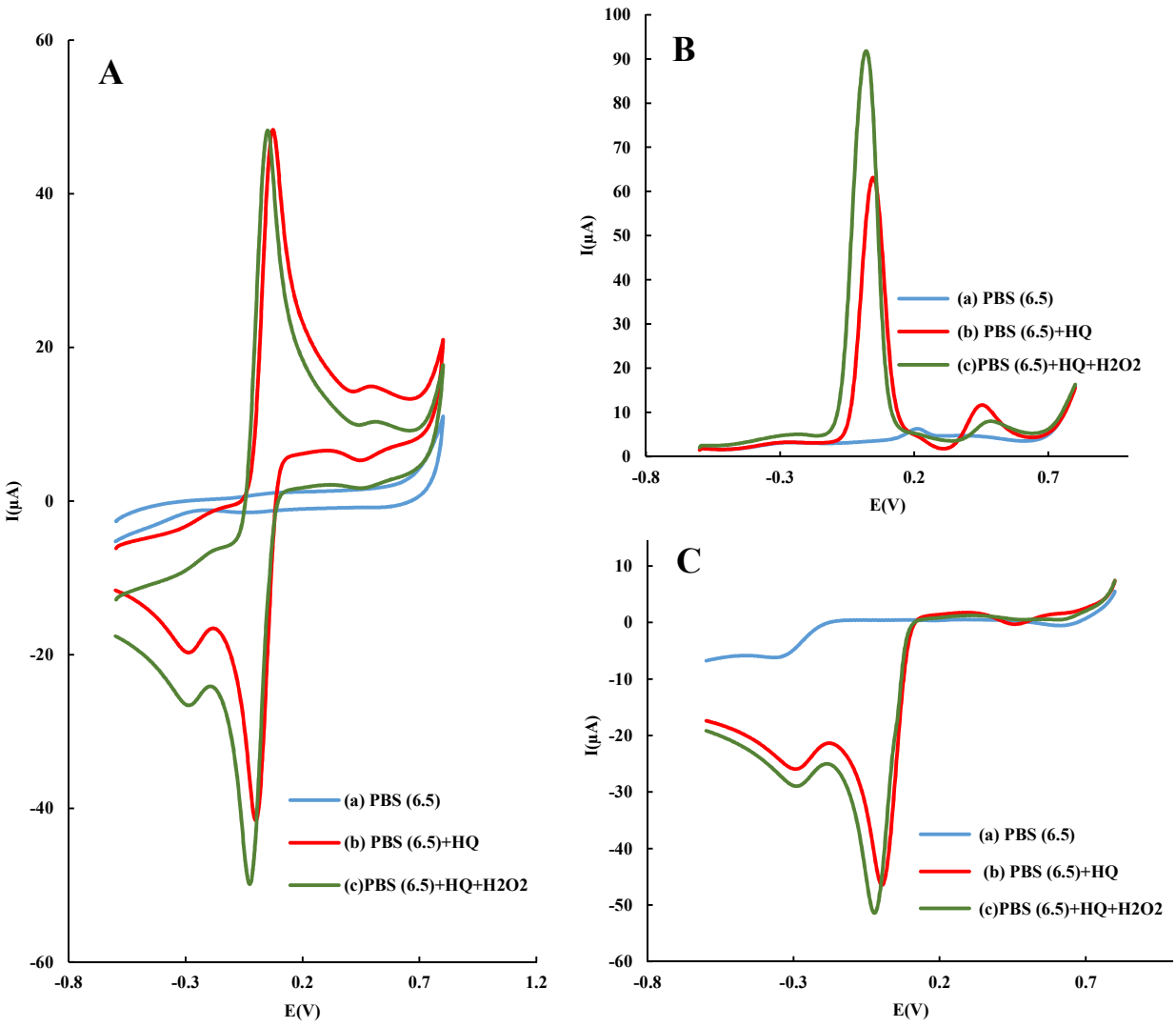

Figure 2

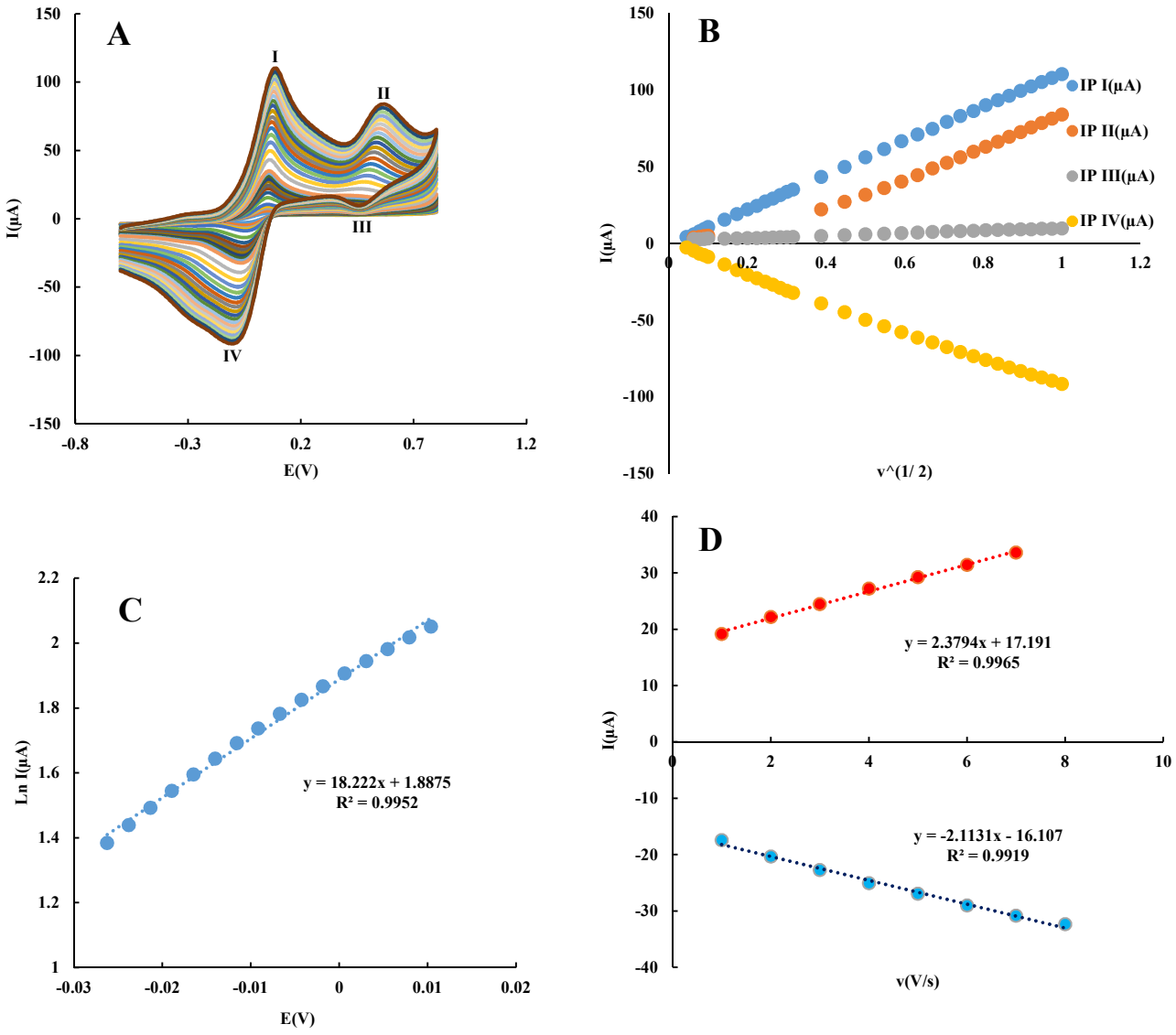

Figure 3

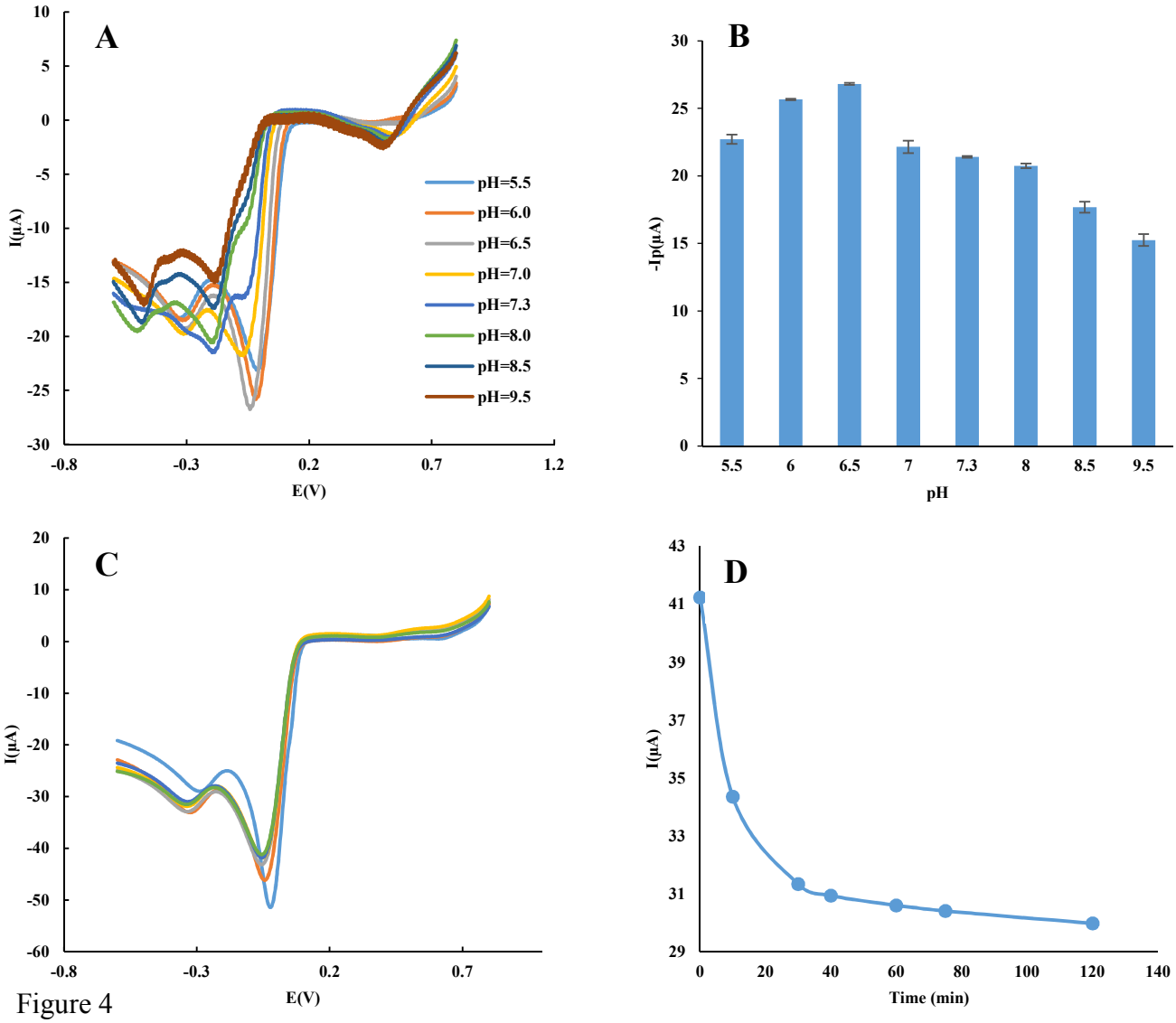

Figure 4

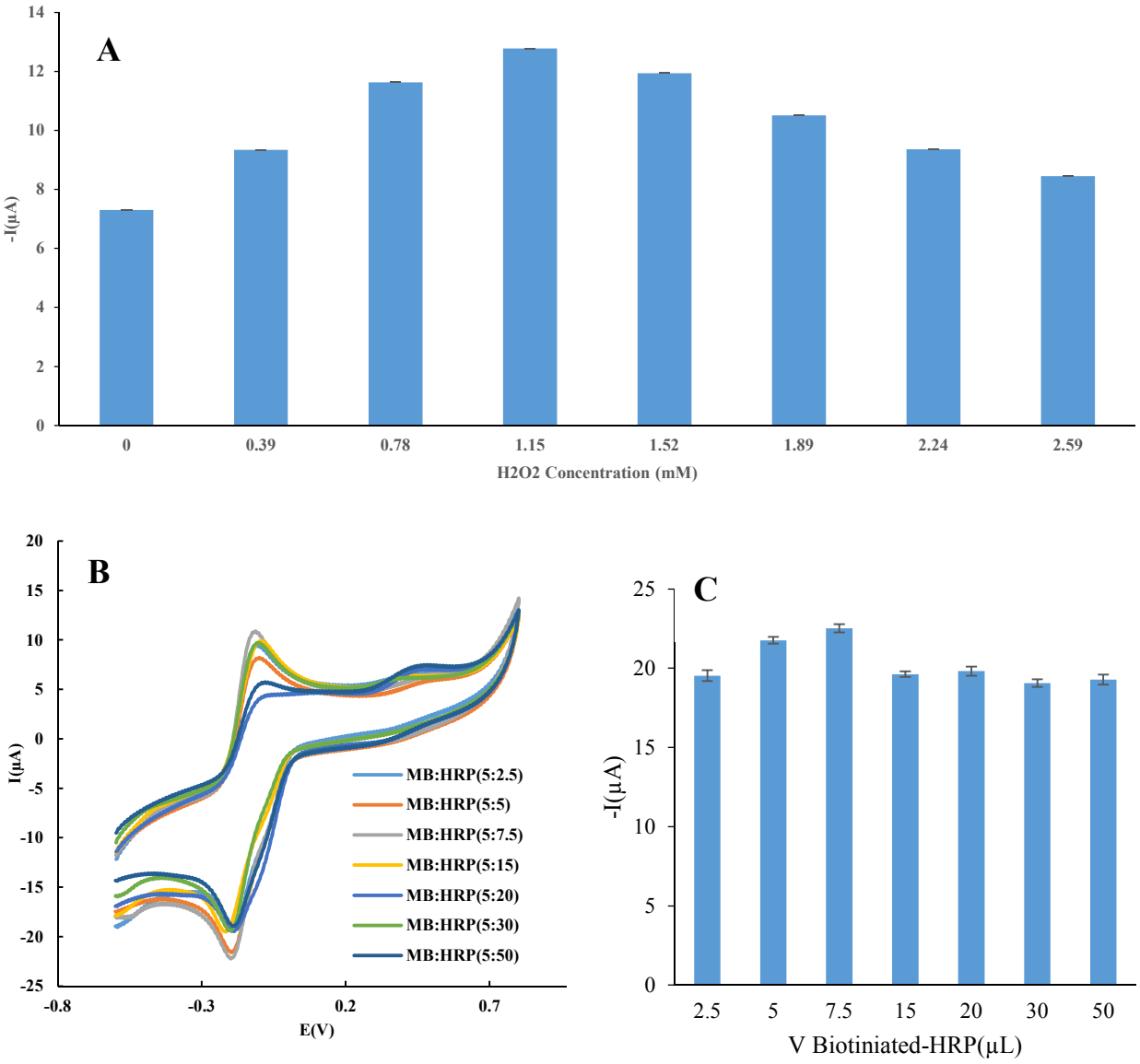

Figure 5

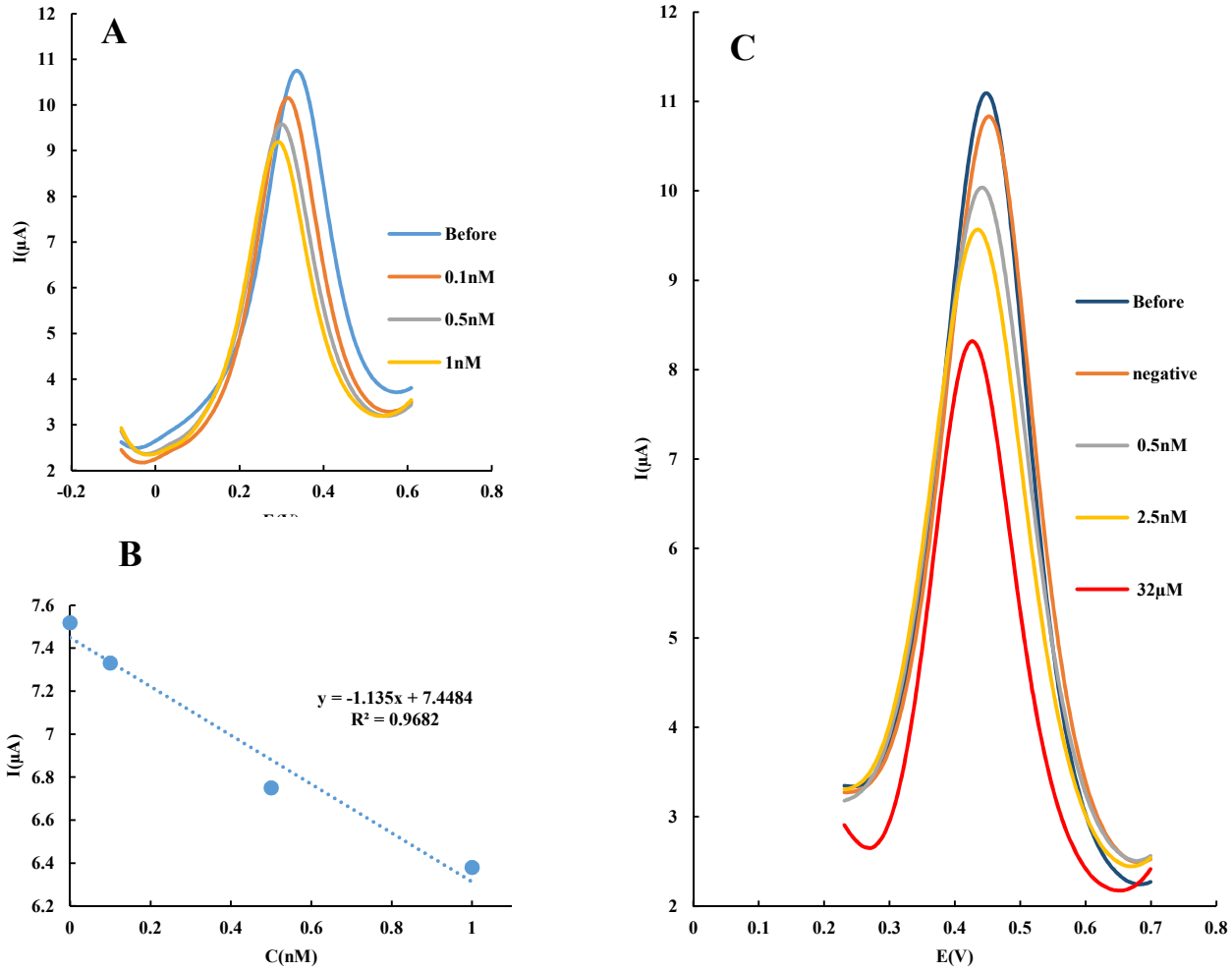

Figure 6

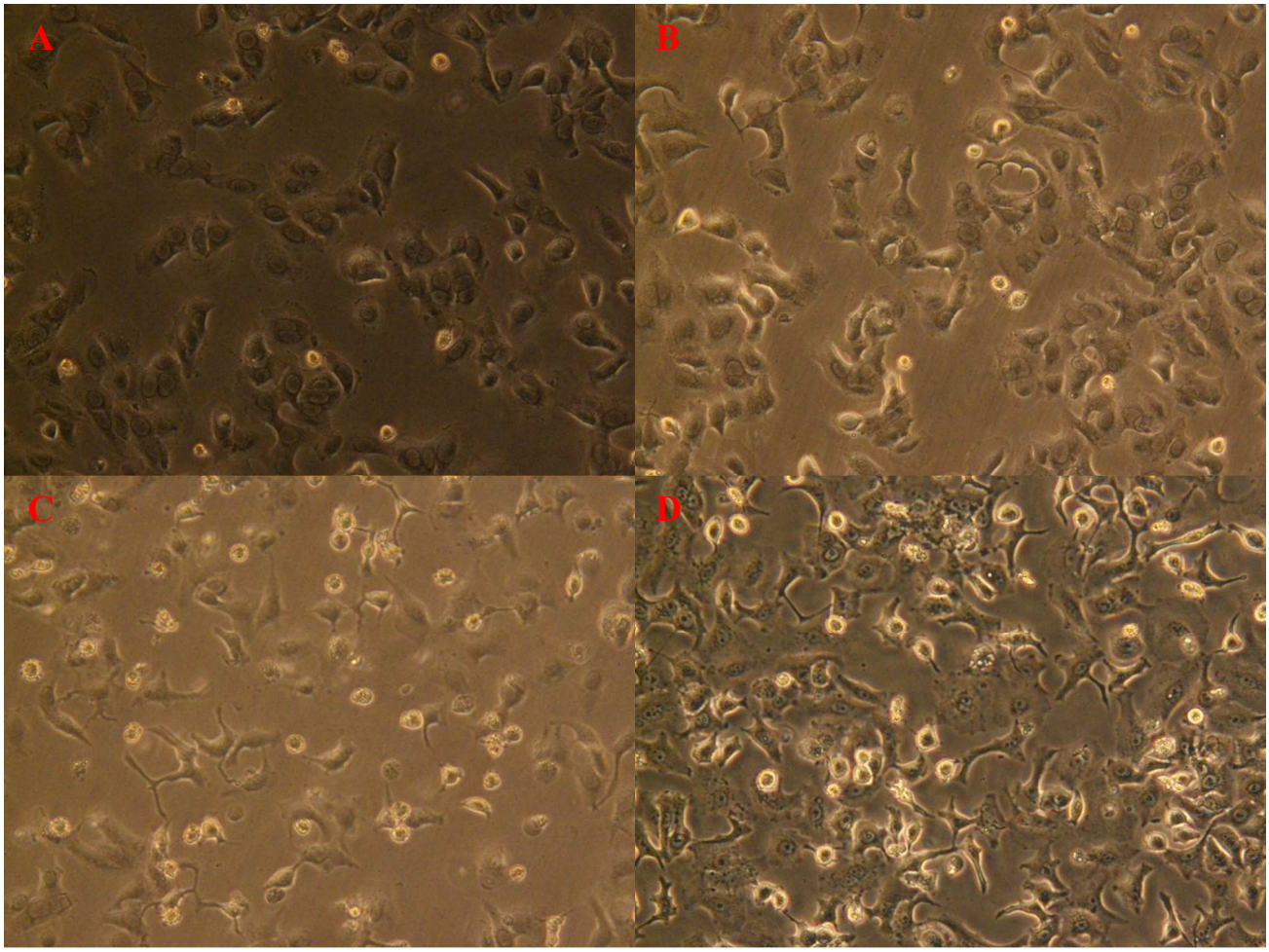

Figure 7

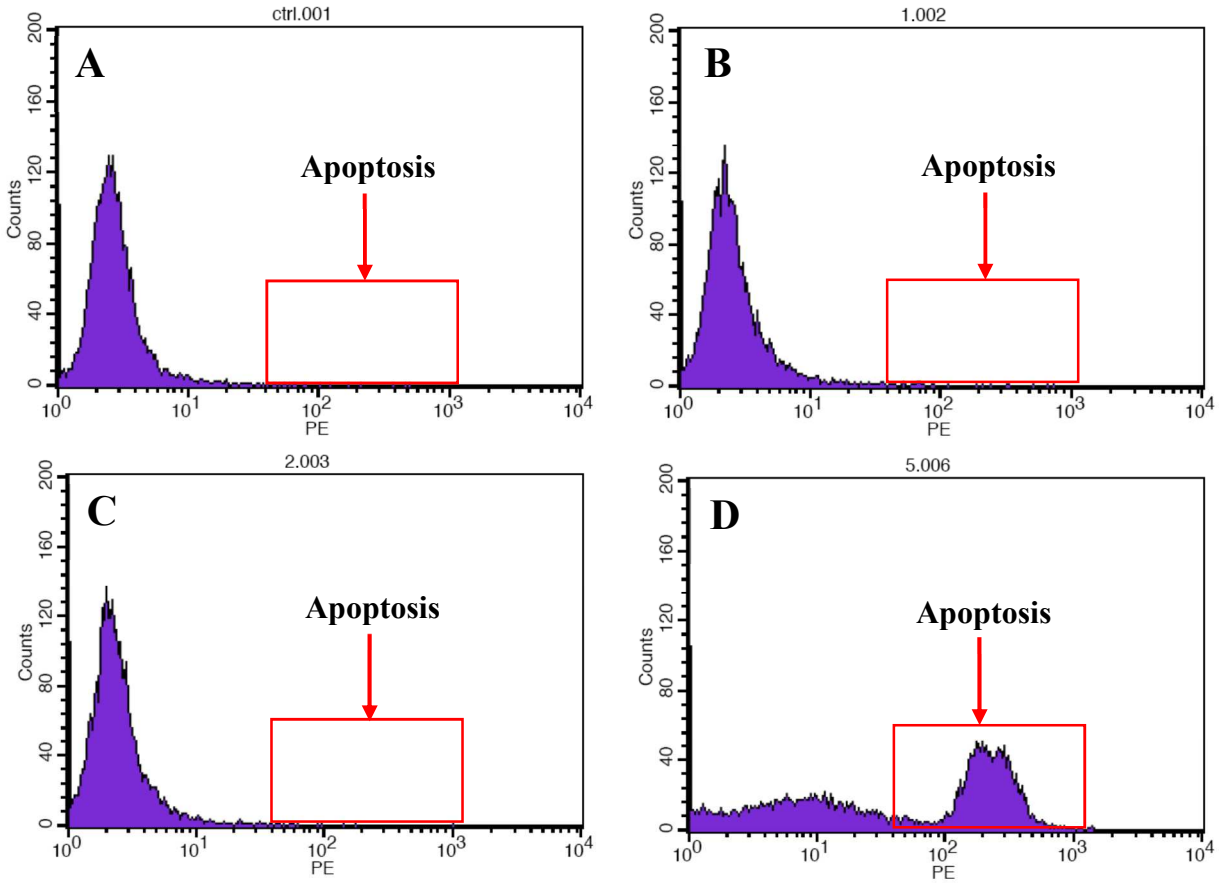

Figure 8

DEVD modifier	LOD**	LDR	Method	Reference
MB-HRP	100 pM	100pM-1nM	SWV	This work*
ferrocene	Not reported	Not reported	CV	[20]
CdTe QD	Not reported	Not reported	ASW	[21]
p-nitroaniline	0.1 nM	0.1nM-10nM	DPV	[23]
SA-ALP	5nM	5nM-50nM	DPV	[24]
AuNPs	0.36nM 0.18nM	0.36nM-5.4nM 0.18nM-7.2nM	colorimetric	[27]
Fluorescein amidite	0.4nM	0.4nM-21.3nM	fluorescence	[30]
green fluorescent protein	3.2nM	3.2nM-80nM	FRET	[32]
QD and Texas Red	Not reported	Not reported	FRET	[33]
p-nitroanilide	50μM	50μM-100μM	Fluorometric and Colorimetric	[34]

* ASV: anodic stripping voltammetry, QD: quantum dots, SA-ALP: streptavidin-labeled alkaline phosphatase, SPR: surface plasmon resonance, AuNPs: gold nanoparticles, FRET: fluorescence resonance energy transfer.
** Limit of detection (LOD) was calculated as LOD=3 times of the blank current (n=10).

Table 1

Graphical abstract